Expansion of cropland area during an abrupt sunlight reduction scenario

Luisa L. Monteiro[1,2,*], Mike Hinge[1], Morgan Rivers[1], Simon Blouin[1], Jacobus Daniel van der Walt[3] and David Denkenberger [1,2,*]

[1]Alliance to Feed the Earth in Disasters (ALLFED) Lafayette, CO 80026, USA

[2]Department of Mechanical Engineering, University of Canterbury, Private Bag 4800 Christchurch 8140, New Zealand;

[3]Department of Civil Engineering, University of Canterbury, Private Bag 4800 Christchurch 8140, New Zealand;

*****Correspondence: luis4lopesmonteiro@gmail.com (L.L.M.)

This is a non-peer reviewed preprint submitted to EarthArXiv, and has been submitted to the Global Food Security journal for peer review.

Abstract: In the eventuality of a major volcanic eruption or nuclear war, particles would accumulate in the stratosphere and reduce sunlight, potentially altering climate conditions severely and decreasing crop yields. Mass starvation could be prevented with the help of resilient foods, such as transforming natural gas into protein, wood into sugar, and relocating crops. One intervention not yet analysed is expanding cropland area by converting other types of land, such as pasture and second-growth forests into land that could be cultivated. We find approximately 515 million hectares would be fit for cropland expansion during a catastrophe. Three land-clearing scenarios were explored: the global-equipment-sharing scenario, in which the area fit for expansion is cleared in 12 months, feeding 39% of the global population by the end of the first year after the catastrophe; the no-equipment-trade scenario, in which 442 million hectares of land are cleared in 7 years, feeding 20% of people by the end of the first year, and the export-pool-equipment-trade scenario, where the supply of extra machinery to a few countries allows for the clearing of 511 million hectares in 7 years, feeding 27% of people by the end of the first year. This project shows the potential to mitigate starvation during catastrophes. By sparing old-growth forests, the impact on biodiversity would be limited and could mitigate desperate humans from hunting species to extinction.

Keywords: food security, resilient foods, global catastrophic risks, existential risks, crop area expansion, nuclear war.

1. Introduction

An abrupt sunlight-reduction scenario (ASRS) occurs when massive amounts of aerosols are released into the stratosphere, remaining there for several years absorbing and or reflecting solar radiation. The aerosols prevent sunlight from reaching the Earth's surface, reducing global temperatures, precipitation, and vapour pressure of water [1], [2]. An ASRS could occur following an asteroid or comet impact, large volcanic eruption, or nuclear war, causing "nuclear winter" (NW) [2]. The probability of a nuclear war between the USA and Russia is ~0.3%/annum [3], this is higher than that of other possible ASRS causes. The detonation of nuclear weaponry would set fire to nearby cities and industrial areas, causing physical destruction, radioactive contamination, and releasing smoke (soot) into the upper atmosphere [4], [5]. While physical destruction would be more prevalent closer to explosion sites, the radioactive materials and soot would rapidly spread across the world upon reaching the stratosphere [6]. The soot accumulates in and absorbs solar radiation from the stratosphere, accelerating the reactions that destroy the ozone layer, increasing the levels of UV radiation at the planet's surface, and decreasing global average temperatures [4], [5], [7].

The severity of global cooling would depend on the number and power of nuclear weapons and the targets. Simulations performed by Coupe et al. [6] showed a temperature decrease of 25 – 30 ^{o}C in the centre of Northern Hemisphere continents would induce hard freezes for the first three years of the catastrophe, while the continents in the tropics would experience a temperature decrease of 5 – 12 ^{o}C. Modelling studies show that a NW could disrupt climate for 5 to 10 years [4], which would cause a massive food system shock on land and in the oceans [8], [9]. Global cooling would severely decrease the yields of current crops, shortening growing seasons in mid-latitude regions and delaying crop maturation [5]. Growing seasons could be less affected in the tropics [4], but higher levels of UV would damage the crops [9]. Lower precipitation levels would also hinder normal crop yields [5], though some regions could experience less water limitation due to low temperatures and high relative humidity. It is uncertain how much soot would be injected into the stratosphere; Xia et al.'s NW simulations show a 5 tera-grams (Tg) soot injection could decrease average calorie production by 7% globally in years 1 – 5 after the conflict [10], which exceeds the largest drop ever recorded by the Food and Agriculture Organization (FAO), while a 150 Tg soot injection could potentially cause a 90% drop in crops' global average calorie production [8].

For a 5 Tg soot injection, 88% of the global population would not starve even if international trade ceased, but this number would decrease with the increase in soot injections [8]. Starvation during a catastrophic event could be avoided by developing resilient food systems to provide food security to the largest number of people possible, while being affordable to the most vulnerable [2]. Rivers et al. [11] analysed the influence of different food system adaptations to prevent starvation during a NW with a soot injection of 150 Tg, which showed only 15% of the population's global caloric needs would be met if trade is interrupted and no adaptations are made, but this could be mitigated by adapting the current food system and producing resilient foods such as seaweed [12], greenhouse crops [13], lignocellulosic sugar [14], methane single cell proteins [15], leaf protein concentrate [16], and synthetic fat [17] to meet the population's

calorie requirements. Wilson et al. [18] looked into outdoor frost-resistant crop growing during ASRSs as a potential food source in New Zealand, which showed that depending on the drop in agricultural production, current cropland may not be enough to feed the country's population. An underexplored resilient food system is the expansion of cropland through conversion of other land types; the drop in food production levels during an ASRS could be rectified by expanding cropland area to other land types to grow cold-tolerant plants, producing more food in a short amount of time, thus mitigating the inflation of food prices and preventing the global population from starving.

Both pastures and forested areas with dead trees could be converted to cropland in NW to mitigate starvation. According to the Global Food and Agriculture Statistics of FAO (FAOSTAT), global pastures occupy an area of 3,360 million hectares (Mha). Conversion of pasture to cropland is considered a form of agricultural intensification with benefits of decreasing deforestation rates, improving soil fertility and climate change mitigation [19]. In a NW, food designated for livestock would be directed towards humans, and some livestock would be killed for human consumption, reducing the need for pasture to feed these animals. FAO's Global Forest Resources Assessment (GFRA) from 2020 states 4,060 Mha of the planet's land area are occupied by forests [20], which would be severely affected by an ASRS. During a NW, temperate zones would experience a severe temperature drop which would cause acute tree death from hard freezes, while surviving trees would suffer from the lack of precipitation and sunlight, the detrimental effects of UV radiation on plant development, and the hindrance of photosynthesis because of soot stuck to leaves [7]. The dead trees could be harvested and used for mushroom or shipworm growth [21], lignocellulosic sugar production [14], or chipped for use in wood gasifiers [22], and the areas formerly occupied by trees could be converted into cropland.

Conversion of pastures driven by crop expansion is a controversial topic, as it reduces the availability of soil organic carbon (SOC) in the first years of cultivation, destroys the soil's aggregate structure, and releases high amounts of CO_2 into the atmosphere. SOC availability is further compromised with higher temperatures, creating positive feedback between SOC depletion and global warming [23]. However, the severe temperature drop during NW could prevent accelerated SOC depletion and emissions of CO_2 could help mitigate global cooling, making the process less contentious. SOC losses could also be mitigated with carbon input in tillage and continuous fertilisation [24], [25]. The same applies to the conversion of forestland, but SOC losses in the conversion of primary forest into cropland are greater than the ones in the conversion of secondary forest into cropland, making secondary forests' SOC less vulnerable to land-use changes [24].

Some deserted areas could also prove useful for cropland expansion. Deserts constitute a fifth of global land area but are rarely used for mass cultivation due to their poor soil and climatic conditions. Desert soil can be turned into arable land by mixing and coating sand granules with a constraining material to make it retain water and nutrients and sustain microorganism growth suitable for cultivation [26], but this process is too expensive for most farmers and has large water requirements [27]. Climate models suggest a NW would cause a temperature drop, a slight increase in precipitation, and increased relative humidity in the Sahara desert, meaning some areas could become hospitable to plant growth. This was the case early in the Holocene epoch,

in which the desert hosted several types of vegetation due to colder weather [28], and it could happen once again in NW, meaning current desert areas could be used to grow crops in advantageous locations.

This work explores the potential of cropland expansion via land conversion as a food-provider system, by quantifying how much cropland can theoretically be expanded, what resources are available to do so, and to what degree is it possible to mitigate starvation during NW.

2. Methods

2.1. Crop model

The Mink global gridded crop model [29], based on the Decision-Support System for Agrotechnology Transfer (DSSAT) physiological crop model, was used to assess winter wheat crop yields in the land to which cropland could be expanded. Mink is a product of the collaborative efforts of the International Food Policy Research Institute and the Consultative Group on International Agricultural Research (IFPRI/CGIAR) and the Alliance to Feed the Earth in Disasters (ALLFED). A single winter wheat cultivar, selected for its tolerance of low temperatures and drought, short vernalization period, and energy density, was modelled based on the crop growth parameters of winter wheat grown in northern Europe. We considered the same planting months for the first 7 years of NW, with current fertiliser and pesticide levels for rainfed cropland. Current cropland, bodies of water, and ice were excluded to assess viable areas for cropland expansion.

The model considered two scenarios: (i) baseline conditions, with relocation of wheat crops to viable non-cropland areas; and (ii) NW conditions, with a 150 Tg soot injection. After calculating the yield for all simulated years and planting months, the best planting month was determined as the single calendar month that maximised the yield over the first 7 years of NW. Overall wheat production of expanded land in each country was the arithmetic mean of the first 7 years of NW.

Two corrections were implemented to improve prediction accuracy: (1) a bias correction to climate data in both baseline and NW scenarios, to match baseline temperature, rainfall, and solar radiation with historical data; and (2) a temperature-dependent correction to reduce DSSAT crop yields at lower temperatures to better match the predictions of independent crop models and historical data [30], [31].

2.2. Land clearing operations

We considered areas fit for expansion should have an average annual wheat yield ≥1000 kg/ha over the grid cell, referring to them as productive areas (PA). Since the model provides details on land coverage, we focused on PA classified as herbaceous vegetation (H), barren land (B), shrubland (S), and forest with trees aged 1 - 10 (F1), 11 - 20 (F2), and 21 - 30 years-old (F3).

The appropriate land-clearing operations are chosen based on factors such as soil conditions, topography and vegetative growth [32]. Herbaceous plants lack a persistent stem and a firm structure, and shrubs are mostly perennial plants less than 5 metres tall [33], with relatively shallow roots. Machines equipped with metal blades can easily uproot these plants, effectively levelling and clearing the area. The same applies to barren land, where land clearing would focus on terrain levelling, grading and debris and rock removal.

When clearing forested areas, factors such as stem density, tree size, and presence of hardwoods must be considered. Trees with a diameter under 20 cm can be removed with dozers and skid steer and compact track loaders, while bigger trees would be easier to harvest with appropriate forestry equipment [32]. After harvesting and removing the stumps and large rocks, the terrain is graded, and levelled and the debris is removed. Subsequently, the land is ready for cultivation, to be ploughed with farm tractors to sow the seeds.

2.3. Machinery

We started by determining what kind of equipment is available to carry out the tasks and how many machine units are available. Levelling and removal of debris (e.g. rocks and shrubs), ploughing, and earth moving are performed by machines often used in construction. We considered machines such as skid steer and compact track loaders to pick up, transfer, and move rocks and debris, and dozers for driving over dense vegetation, ground-levelling, and rock removal [34].

Construction machines (construction equipment) can be used alongside forestry machines to remove trees and prepare the ground for agriculture. Small trees can be uprooted with dozers, skid steer loaders and compact track loaders, and removed from the area with skidders and forwarders [35]. **Table S1** in the Supplement lists the land clearing operations and the types of machines used in each.

Since there is intersection in the equipment used for land clearing and forestry, we stipulated that the land clearing process begins in lands with less vegetation, and only progresses to lands with more and larger forms of vegetation when the previous areas have been cleared.

Global machine availability, as shown in **Table 1**, was calculated by multiplying the number of units of a given machine sold annually by the effective life of that machine. Since international trade interruptions are likely, it is crucial to determine each country's machinery fleet to assess their capacity for expanding their own cropland. We estimated each country's construction machinery fleets according to the country's contribution of construction to the global gross domestic product (GDP), and forestry machinery fleets according to the country's contribution to global roundwood production. We assumed the distribution of equipment types would remain constant, for example , since 1.2% of the global construction machinery fleet is made up of dozers, 1.2% of each country's construction machinery fleet consists of dozers.

Table 1 - Global number of construction and forestry machines.

Type	Machine	Global number of units	Average productivity of the machine	Ref
Construction	Skid steer loaders	294,000	1.2 ha/day	[36]
	Compact track loaders	8,250,000	1.2 ha/day	
	Dozers [a]	448,000	19 ha/day	[32]
			13 ha/day	
Forestry	Forwarders	858,667	151 m^3/day	[37], [38]
	Skidders	197,989	450 m^3/day	[39], [40]

a) Dozer productivity was calculated according to the Caterpillar Performance Handbook, which changes according to the type of vegetation present in the land to be cleared. Assuming a stem density < 990 stems/ha, hardwood presence of 0-25% and 25-75% results in a productivity of 19 and 13 ha/day, respectively. The latter is considered for forest clearing, while the former is used for levelling and clearing land with small forms of vegetation.

Fleet productivity was calculated by multiplying that machine's average productivity by the number of available machines. The productivity of each task was calculated by adding the productivity of the global fleet of machines used in that task. The time taken to clear each land type was calculated by dividing the amount of area to be cleared by the productivity of the land clearing tasks. For forested areas, the time was calculated by dividing the forested area to be cleared by the productivity of the land clearing tasks, but the time required to remove the trees from the area was calculated by dividing the volume of the stems and crowns by the productivity of skidders and forwarders. We assumed the time required to clear a forested area would equal the time of the longest task. A working day of 8 working hours, 7 days per week was assumed.

2.4. Forest age distribution and tree measurements

The rate at which forested land is cleared is a function of tree measurements, which is itself a function of the species, environment and age of the trees. A global forest age dataset (GFAD) developed by Poulter et al. [41] from country-level forest and biomass inventories from 2000 - 2010 provided the area occupied by trees belonging to different age groups. The GFAD was used to estimate the age distribution of the PA located by the crop model, and a linear interpolation was used to conciliate the resolution difference between the GFAD and crop model datasets. A stem density of 600 stems/ha was assumed based on stem density of forests in tropical moist regions [42].

The basic dimensions (height and diameter) of trees were estimated based on the dimensions of each continents' most common trees (see **Equations S1 to S9** in the Supplement). Averaged measurements from trees of the *Brachystegia* and *Julbernardia* genera were used for Africa, and averaged measurements from trees of the *Picea* and *Nothofagus* genera were used for America. *Pinus* was used for both Asia and Europe, while *Eucalyptus* was chosen for Oceania. Averages of these diameter and height measurements were used to estimate other data such as

tree volume, crown volume, stump volume, and stump hole volume (see **Equations S10 to S14** in the Supplement). While this is not a precise representation of trees across the world, it serves as a relatively accurate estimate ensuring consistency of crudeness

Since the target areas are F1, F2, and F3, we assumed the average tree age of these areas was 5, 15, and 25 years old, respectively. The measurements of trees at those ages are shown in **Table 2**.

Table 2 - Estimate measurements of trees in the age ranges 0 - 10, 11 - 20, and 21 - 30 years old.

Tree age groups	**1 - 10 years**	**11 - 20 years**	**21 - 30 years**
DBH (cm)	4	11	17
Height (m)	4	10	14
Tree volume (m^3)	0.01	0.09	0.34
Crown volume [b] (m^3)	0.1	0.7	1.6
Stump volume (m^3)	3.0E-04	5.0E-03	1.9E-02
Stump hole volume (m^3)	0.01	0.07	0.19

b) The solid volume of the tree crown was approximated to 3% of the volume of a cone, while tree volume corresponds to the volume of the trunk which is mostly solid, approximated to that of a cylinder, hence the difference in magnitude. Detailed descriptions of how these volumes were calculated are present in the Supplement.

2.5. Land clearing rates

The land clearing process depends on the machinery fleet of each country, land type, and amount of PA to clear. To assess how cleared land increases, we calculated how much area from each different land type is cleared as a function of time for each country according to their machinery fleets. To build the land clearing curves, we assumed land was cleared sequentially, with a rate corresponding to the land type being cleared at a given time. Therefore, each land clearing curve can be split into 4 sections:

1. Herbaceous vegetation, barren, and shrub (HBS);
2. Forest with trees aged 1 - 10 years-old (F1);
3. Forest with trees aged 11 - 20 years-old (F2);
4. Forest with trees aged 21 - 30 years-old (F3).

Each section can be described by the following equations:

$For\ 0 < t \leq t_{HBS} :\ A\ (t)\ = m_{HBS} \times t$ Equation 5

$For\ t_{HBS} < t \leq (t_{HBS} + t_{F1}) :\ A\ (t)\ = m_{F1} \times t + b$ Equation 6

$For\ \ (t_{HBS} + t_{F1}) < t \leq (t_{HBS} + t_{F1} + t_{F2}) :\ A\ (t)\ = m_{F2} \times t + c$ Equation 7

$For\ (t_{HBS} + t_{F1} + t_{F2})\ < t \leq (t_{HBS} + t_{F1} + t_{F2} + t_{F3}) :\ A\ (t)\ = m_{F3} \times t + d$ Equation 8

Where m_{HBS}, m_{F1}, m_{F2}, and m_{F3} correspond to the land clearing rates in ha/day for HBS, F1, F2, and F3, respectively, and t_{HBS}, t_{F1}, t_{F2}, and t_{F3} correspond to the time in days required to clear all the PA of HBS, F1, F2, and F3, respectively. The constants *b*, *c*, and *d* in ha correspond to the points where the land type changes, and are the described by the following equations:

$$b = t_{HBS} \times (m_{HBS} - m_{F1}) \quad \text{Equation 9}$$
$$c = t_{F1} \times (m_{F1} - m_{F2}) + b \quad \text{Equation 10}$$
$$d = t_{F2} \times (m_{F2} - m_{F3}) + c \quad \text{Equation 11}$$

2.6. Wheat production

We stipulated that land cleared in a month is immediately cultivated, and wheat is harvested from that area 8 months after cultivation, which we considered a conservative average since harvest could happen 4 to 12 months after clearing. Then, the land lies fallow for 3 months before being cultivated again. As the amount of available land cleared increases over time, so does the amount of wheat produced every 12-month cycle. This means the area cleared in month 2 is only harvested by month 10, and then again in month 22, along with the area cleared in month 14. Therefore, the wheat produced in month 22 is the sum of the wheat yielded by the lands cleared in months 2 and 14. The amount of wheat produced monthly for each country is calculated by multiplying the area cleared 8 months prior by the average annual wheat yield of that country during NW.

Once we know how much wheat is produced monthly on a global scale, we calculated what percentage of the global population could be fed, assuming a daily intake of 2100 kcal/person and 12% food waste (which is expected to be lower due to increased food scarcity) [14], [15].

2.7. Scenarios

In this work, we aim to assess how cropland expansion and wheat production rates on a global scale can be affected by the distribution of equipment across the world. To this end, we evaluate three scenarios of equipment trade where the geographical distribution, numbers, and availability of the equipment vary. All scenarios assume food trade is maintained (although it is highly likely food trade will collapse if equipment trade collapses) and that equipment is operated 56 hours/week.

2.7.1. Global equipment trade

In this ideal scenario, we assume all the machines in the world are used to clear all the new PA as if it is one combined region. It assumes machines are fully mobile within and between countries. This scenario is referred to as the global trade scenario (GTS).

2.7.2. No-equipment trade

In this scenario, each country relies solely on the equipment within its borders to clear its respective PA, assuming that machines are fully mobile within the country they belong to and that PA within a country is one combined region. It is assumed a country's machinery is focused on land clearing, but since the equipment is assumed to only be operating 56 hours/week, other tasks could be performed with multiple shifts. This scenario is referred to as the no-trade scenario (NTS).

2.7.3. Equipment trade with export pool

We developed an export pool (EP), a machinery inventory comprising machines loaned by several countries without PA that other countries with less machinery can tap into to increase their fleet, making the land clearing process faster. We stipulated countries without PA loan 30% and 40% of their construction and forestry machines to the EP, respectively. It is also assumed the machinery distribution is maintained constantly after this loan, according to the fraction occupied by each equipment type in the global machinery stock. This scenario is referred to as export-pool scenario (EPS).

The number of machines loaned by continent to the EP is shown in **Table S2** in the Supplement. It could be argued these countries could loan a bigger sum of machinery to the EP, but the machinery they own could still be used to carry out other tasks that require machine power. The EP equipment is then distributed across the countries that take over 3 years to clear their PA in NTS, according to how much area those countries have to clear (see **Table S3** in the Supplement), to speed up their land clearing process. Each country receives the same fraction of construction and forestry equipment, and the machines' productivity, clearing times, land clearing curve factors, and monthly wheat production are recalculated. The equipment is distributed before the clearing process begins, and the machines placed in a country are not moved to other countries once the clearing in the country where they were placed is done.

3. Results and discussion

3.1. Crop model and machinery

The crop model allowed the visualisation of overall wheat yields in non-cropland regions in baseline and NW conditions over the course of 7 years, as seen in **Figure 1**. **Table 3** shows how much PA is available in each continent in baseline and NW conditions, showing a 60% drop in PA, and the average wheat yields of PA in both conditions, registering a 54% drop in NW.

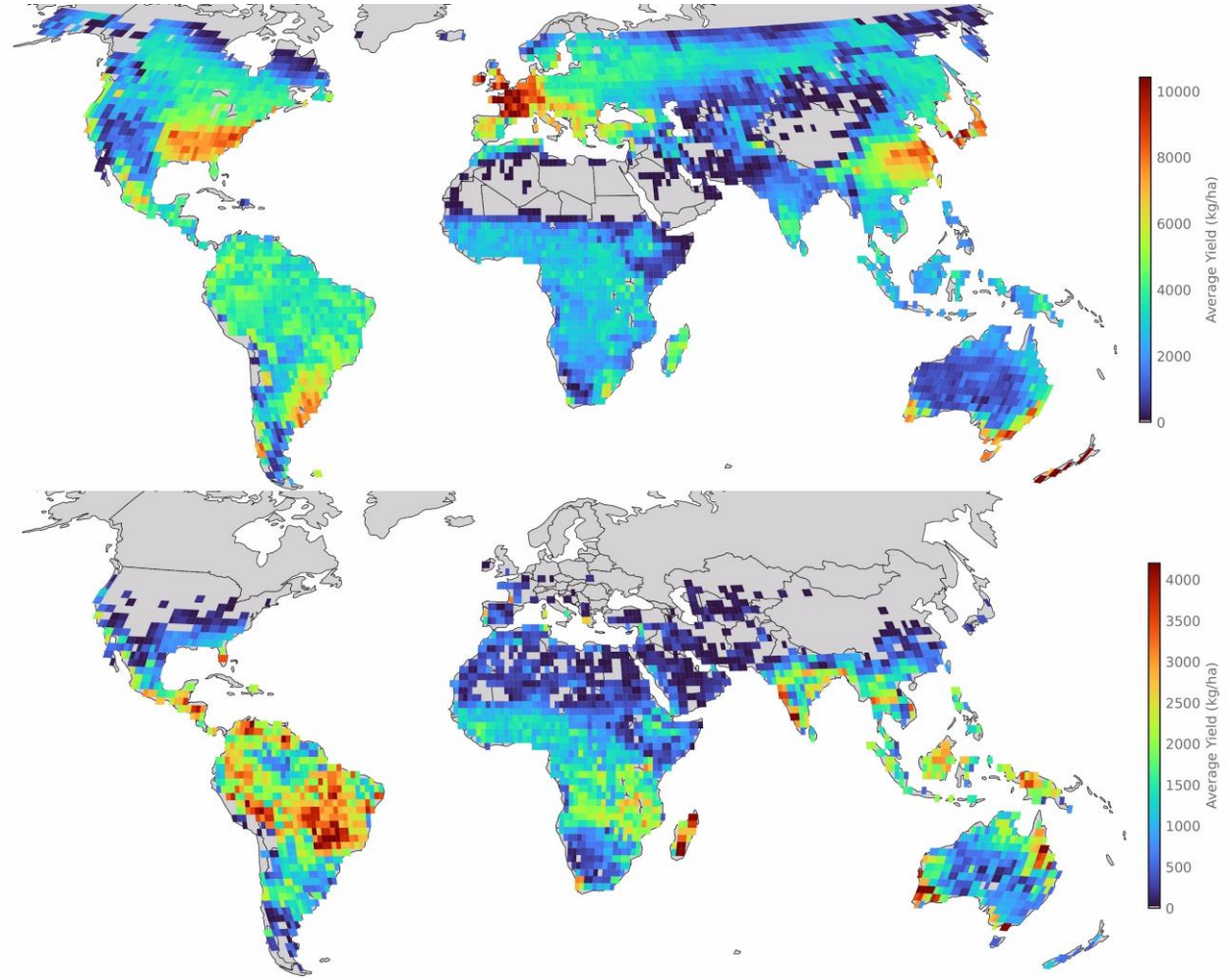

Figure 1 - Crop yield (in kg/ha) heat maps for baseline (top) and nuclear winter conditions (bottom). Note the reduced scale for nuclear winter. Grey areas correspond to fully occupied areas or with no yield.

Table 3 - Productive area outside current planted area and average in each continent.

	Productive area (Mha)		**Average annual wheat yield of PA (kg/ha)**	
Continent	**Baseline conditions**	**NW conditions**	**Baseline conditions**	**NW conditions**
Africa	655	388	2,442	1,432
America	1,156	570	3,209	1,784
Asia	457	118	2,125	1,459
Europe	514	2	3,726	1,376
Oceania	212	114	3,090	1,567
World	2,994	1,193	2,842	1,539

The PA covered in the selected land types corresponds to 43% of the global PA in NW conditions. Of the 153 countries modelled, only 73 have PA of the selected land types. **Figure 2** shows the PA per continent according to land cover type.

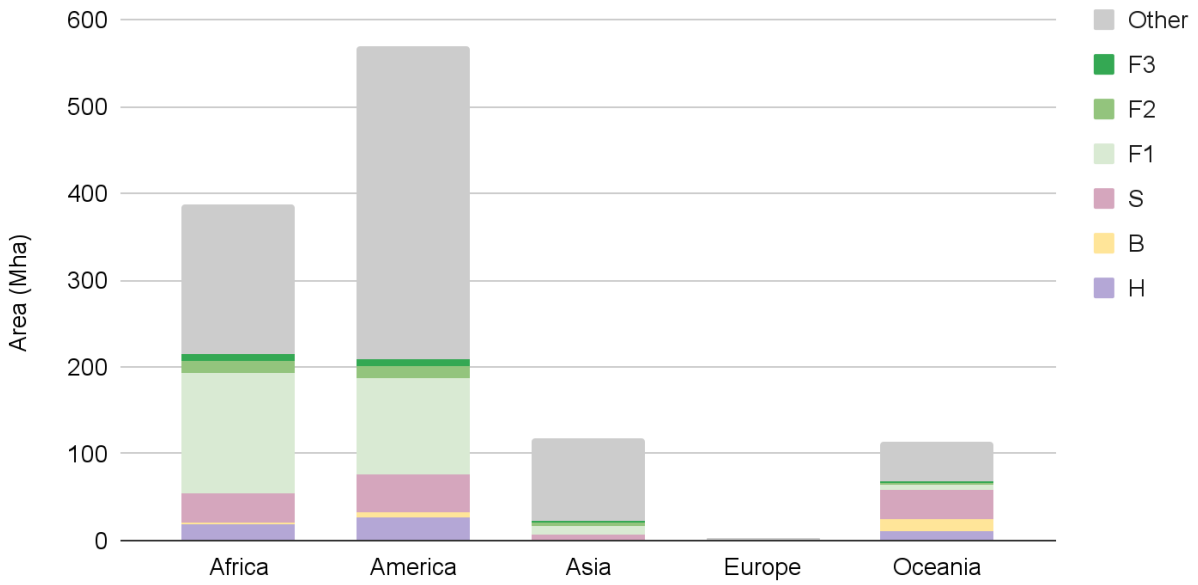

Figure 2 - Productive area in NW according to land cover type

With the crop model, it is possible to quantify just how detrimental the alteration in climate conditions is to crop yields and PA. Europe, Asia and America show the sharpest decline in PA, while Africa and Oceania experience the smallest drops in new PA (losses of 41% and 46%, respectively). This is in agreement with Xia et al. 's model, where Northern Hemisphere extratropical countries are the most affected while countries in the tropics suffer a less extreme temperature drop, allowing them to maintain a good crop yield [8]. More than half of the PA of selected land types is classified as F1, constituting the biggest fraction of PA in Africa and America during NW. Areas covered in shrub represent nearly a quarter of the selected global PA, accounting for 23% of the PA from the selected land types of Oceania. This makes young forest and shrubland the land types with the biggest potential for cropland expansion.

As for machinery, we estimated there would be approximately 38 million and 3 million units of construction and forestry machines, respectively. **Table 4** details the top 10 countries with the biggest PA and their respective machinery fleets.

Table 4 - Top 10 countries with the highest amount of productive area available for cropland expansion of the viable land types and their respective equipment fleet

		Number of equipment units				
Country	**Productive area (Mha)**	*Skid steer loaders*	*Compact track loaders*	*Dozers*	*Forwarders*	*Skidders*
Brazil	94	4383	122980	6678	66221	15269
Australia	66	5134	144053	7823	6513	1502

Democratic Republic of Congo	34	340	9552	519	20628	4756
Angola	34	529	14835	806	1402	323
Argentina	29	1684	47258	2566	4158	959
Zambia	19	107	2989	162	5604	1292
Bolivia	17	127	3568	194	883	204
Tanzania	17	231	6491	352	6263	1444
Mexico	16	5431	152395	8276	10002	2306
Mozambique	14	46	1298	71	4075	940

3.2. Land clearing scenarios

We calculated land clearing rates and times for each of the different land types in each country to determine how much area is cleared globally, thereby determining how much cropland area could be expanded each year. We stipulated land clearing would only start one month after the catastrophe occurred, as the first month is dedicated to assessing the catastrophe and transporting machinery to places where it is needed. **Figure 3** depicts the land clearing process in different equipment-trade scenarios, and **Figures 4** and **5** depict how much wheat is produced per month from the expanded area and how many people can be fed per month according to the wheat produced per cycle, respectively.

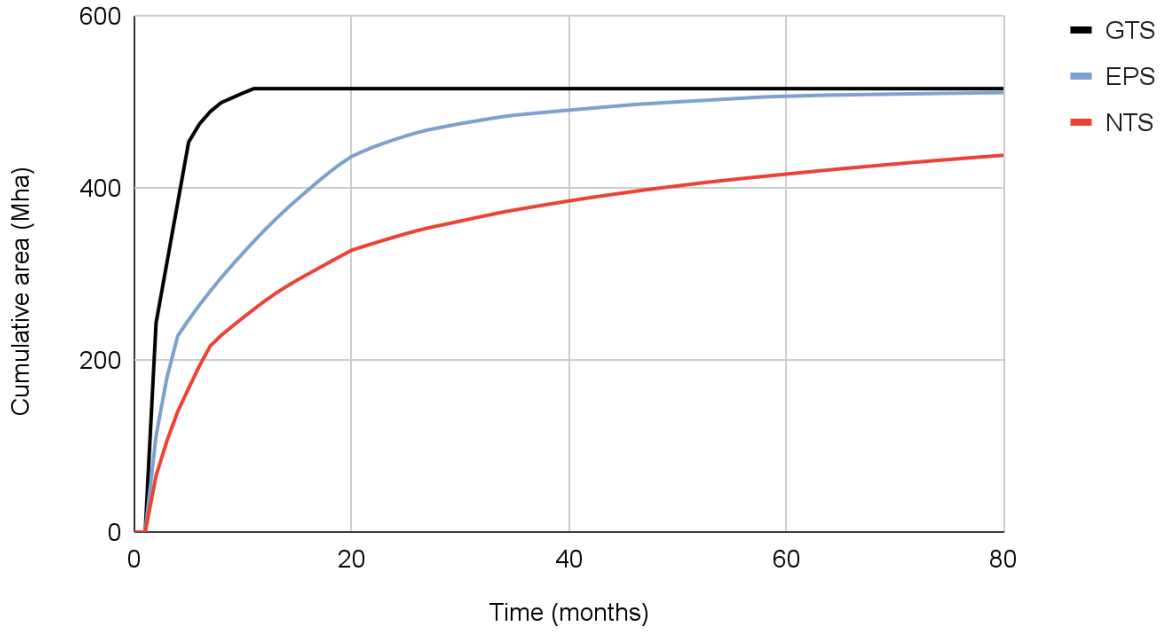

Figure 3 - Comparison of the land clearing process with different equipment-trade scenarios.

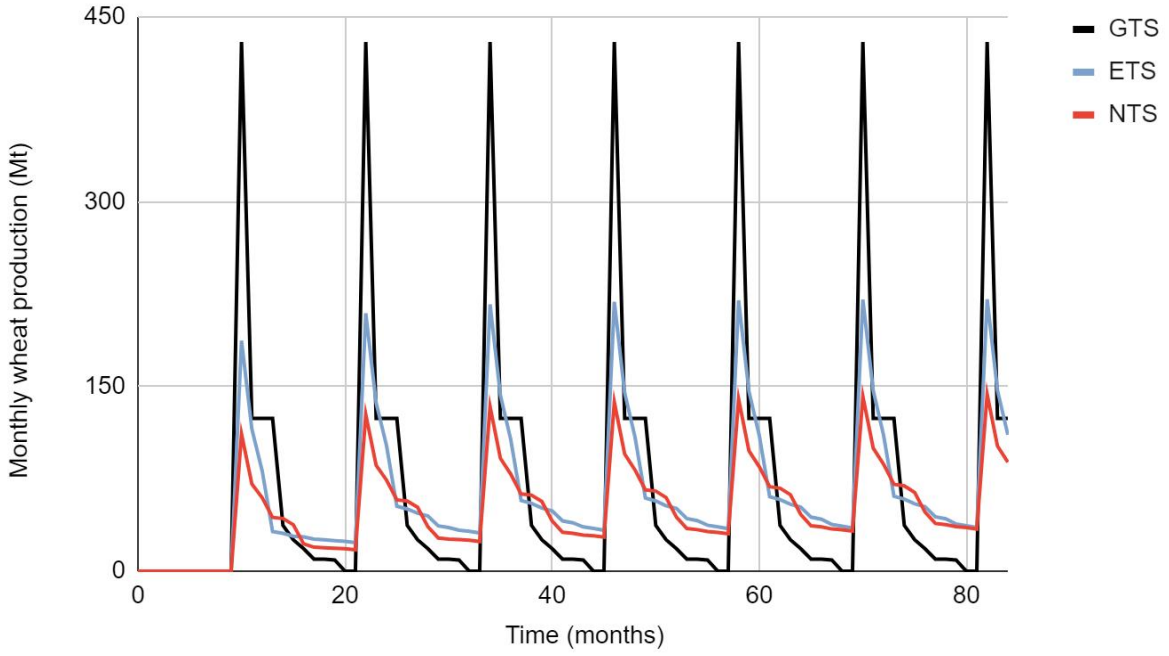

Figure 4 - Monthly wheat production in million tons (Mt) in different equipment-trade scenarios.

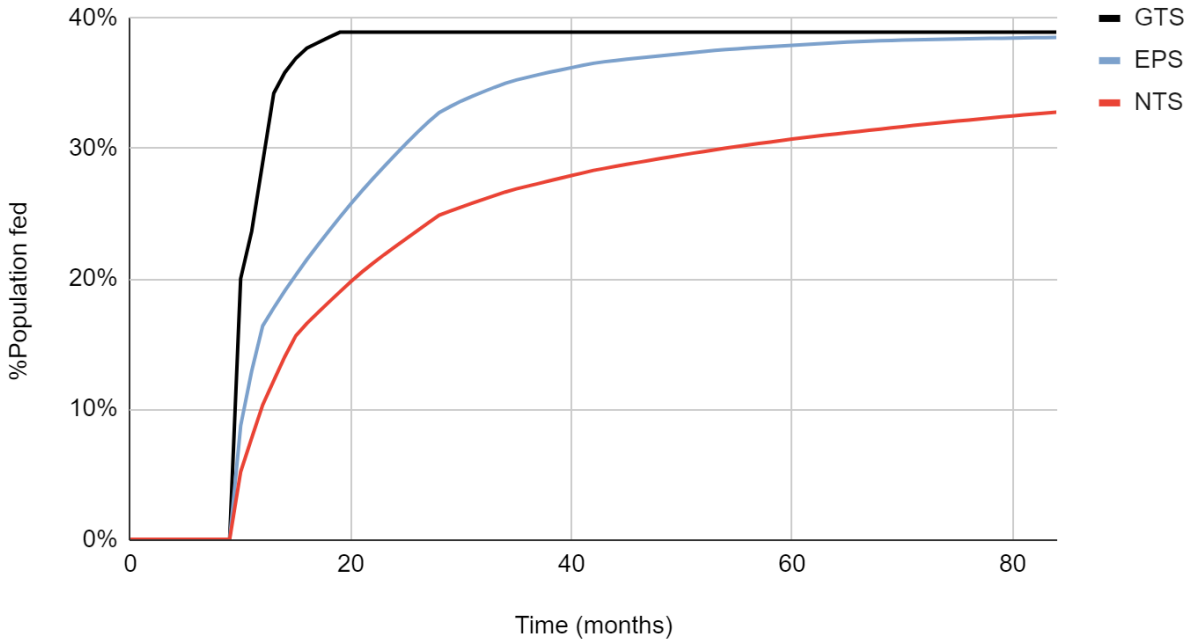

Figure 5 - Monthly global food demand met by the different equipment-trade scenarios smoothed over 12 month periods.

3.2.1. Global equipment trade

In **Figure 3**, in the GTS, with perfect machine allocation, all 515 Mha of new PA of the selected land types are cleared in a year (with most of it happening in the first 8 months), expanding cropland area by 33%.

For the wheat production, a weighted average of the average annual yields of each country was used to calculate the wheat produced from the cleared area. From the second year onwards, each wheat production cycle (a 12-month period) would yield approximately 911 million tons (Mt) of wheat (**Figure 4**), corresponding to an average monthly wheat availability of 75 Mt of wheat, which would feed on average 39% of the global population throughout the year starting from month 18 of the catastrophe, as depicted in **Figure 5**.

With current wheat cropland area (approximately 215 Mha [43]) and climate, approximately 780 Mt of wheat/year are produced [44] (3.63 t/ha/year). In the GTS, it would be possible to produce approximately 870 Mt of wheat per chronological year from the expanded area (1.70 t/ha/year) over a 7-year period, which would exceed current annual wheat production by 13%. This average accounts for the initial ramp-up period and subsequent full production cycles.

3.2.2. No equipment trade

Compared to the GTS, land clearing in NTS happens at a much lower rate (**Figure 3**), as 7 years aren't enough to clear all the PA of the selected land types. **Table 5** depicts how much the expanded area increases per continent annually in the NTS, showing that expansion happens quickly in the first 4 years, after which it slows down as more than half of the countries have cleared their land. Europe is the first continent to clear its land, as there are only 4 countries with new PA, while Africa takes the longest because of limited numbers of construction and forestry machines. By year 7, only 442 Mha of land have been cleared globally, which is 86% of the global PA of the selected land types and corresponds to a cropland area expansion of 28%.

Table 5 - Cumulative expanded cropland area by year for the no-equipment-trading scenario.

	Total PA cleared (Mha)						
Year	**1**	**2**	**3**	**4**	**5**	**6**	**7**
Africa	57	82	101	117	130	142	152
America	125	172	185	191	194	197	198
Asia	23	23	23	23	23	23	23
Europe	0.90	0.90	0.90	0.90	0.90	0.90	0.90
Oceania	63	66	67	67	67	67	67
World	268	343	376	399	416	430	442

Table 6 shows how much wheat is produced annually in each continent and globally during NW in the NTS from the expanded area. The Americas produce over 2,300 Mt of wheat over the course of 7 years, while Europe produces approximately 8 Mt of wheat (the least among continents). Oceania would be the second biggest wheat producer during the first year of NW, but is surpassed by Africa in the following years. The first production cycle relies on the wheat produced from lands cleared all over the world between months 2 and 13, which would feed on average 5 - 21% of the global population monthly between months 11 and 22 with smoothing. By the fifth cycle, 30% of the global population would be fed every month from the expanded area (**Figure 5**).

Table 6 - Annual wheat production for the no-equipment-trading scenario.

	Annual wheat production (Mt)							
Year	**1**	**2**	**3**	**4**	**5**	**6**	**7**	**Total**
Africa	35	98	132	160	184	204	221	1,034
America	128	290	363	383	394	401	405	2,364
Asia	32	40	40	40	40	40	40	271
Europe	1.18	1.24	1.24	1.24	1.24	1.24	1.24	9
Oceania	46	97	99	100	101	101	101	643
World	242	526	635	684	719	746	768	4,320

Compared with the GTS, the wheat produced from the expanded area over 7 years in the NTS decreases 29% (**Figure 4**). Over 4,000 Mt of wheat are produced globally from the area cleared in 7 years, which corresponds to 620 Mt of wheat produced per chronological year (1.40 t/ha/year), and to 79% of the current annual wheat production. Countries without new PA could rely on current planted area (preferably with crop relocation to more favourable locations), food storage, culled animals, and grazing food production, or produce other resilient foods. Upkeeping food trade would also ensure these countries receive wheat from producing countries during the catastrophe.

3.2.3. Equipment trade with export pool

With 80 countries without new PA in NW that loan part of their equipment to the EP, the land clearing rate in the EPS happens at a faster pace than in the NTS, but not as fast as in the GTS (**Figure 3**). **Table 7** depicts the annual increase of expanded area in each continent in the EPS.

Table 7 - Cumulative expanded cropland area by year for the equipment-trade-with-EP scenario.

	Total PA cleared (Mha)						
Year	**1**	**2**	**3**	**4**	**5**	**6**	**7**
Africa	125	181	196	205	211	212	213

America	137	188	201	204	206	207	207
Asia	23	23	23	23	23	23	23
Europe	0.90	0.90	0.90	0.90	0.90	0.90	0.90
Oceania	65	67	67	67	67	67	67
World	351	460	488	501	508	510	511

The increased land clearing rate relative to NTS would promote an increment in monthly wheat production and in the amount of people fed. Approximately 350 Mha are cleared globally in year 1, while in NTS it would take 3 years to do so. The impact of the EP is mainly noticeable in Africa, America and Oceania; African countries receive 55% of the EP's machinery, but Australia receives the biggest individual fraction of equipment (19%). In NTS, the African continent would have only 150 Mha of cleared area by year 7, while in EPS 213 Mha of PA in Africa are cleared in 6 years. The number of countries capable of clearing their new PA in its totality within 3 years increases from 42 to 58, and 69 countries clear their PA within 7 years, showing how beneficial equipment loaning can be to the execution of this project.

Table 8 shows how much wheat is produced annually in the EPS. The wheat production cycle stabilises by month 60, by which most of the PA has been cleared (**Figure 4**). Over 1,900 Mt of wheat are produced in Africa over 7 years, nearly double what is produced in NTS, while America and Oceania's wheat production increases by 8% and 7%, respectively. With the EP, global wheat production registers a 26% increase compared to the NTS, feeding 4 - 8% more people in the first five years of NW. From the fifth production cycle onwards, it would be possible to feed on average 38% of the global population (**Figure 5**), highlighting how crucial the role of food trade is in preventing widespread famine during a NW.

Table 8 - Annual wheat production per continent with the implementation of EP.

	Annual wheat production (Mt)							
Year	**1**	**2**	**3**	**4**	**5**	**6**	**7**	**Total**
Africa	104	234	293	312	324	332	334	1,934
America	157	317	395	416	422	425	427	2,558
Asia	32	40	40	40	40	40	40	271
Europe	1.18	1.24	1.24	1.24	1.24	1.24	1.24	8.61
Oceania	89	99	101	101	101	101	101	691
World	384	691	830	869	888	898	902	5,462

Wheat production in countries that receive machinery from the EP are shown in **Table S4** in the Supplement, further highlighting the effect of the EP. For example, the wheat production in the EPS in the Central African Republic increases by a factor of 15 relative to the NTS. The EP

proves to be crucial to increase wheat production rates and ensure people have a reliable and affordable food source during a catastrophe, preventing mass starvation.

4. Limitations

Conversion of forests into cropland is often avoided, but since NW would cause acute tree death in many regions, forested regions become targets for land conversion, as those areas can be used to grow crops, minimising the impact on biodiversity by focusing on secondary forests. Replacing a dead forest with living crops could increase transpiration, promoting more precipitation. How much precipitation increases is unknown, but if it is greater than predicted by the climate model, it would help biomes' recovery from the catastrophe. This project could even help with species preservation, as a reliable food source to feed everyone could reduce the pressure on animal hunting during the catastrophe. After the catastrophe, the cleared land would no longer be needed to feed the people and livestock, so it could be rewilded or used to increase production of biofuel, natural fibres, wood for construction, etc.

The global gridded model used in this paper has been validated against current climate for spring and winter wheat. Past validation of the model has shown a Root Mean Square Error (RMSE) globally of 1.3 t/ha for yield and 2.2 Mt/country for country production. We used the CROPSIM-CERES model in DSSAT v4.7.5.11, but this was done for a single cultivar rather than a multi-cultivar ensemble in Gbegbelegbe et al. [45], meaning the yield predictions for baseline climate may be less accurate. We determined this was not a major decrease in yield prediction accuracy, due to the high uncertainty of local climates in NW.

Another uncertainty is the implemented corrections may not have the same bias in NW conditions. Even if the climate bias remains unchanged in NW, climate model predictions may not accurately reproduce the spatial or temporal dynamics in NW conditions, so the forecasts given to farmers in a NW would have significant uncertainty. In addition, yield is likely to be lower for the farmers who need to grow a crop they are inexperienced with, and crop yield tends to be lower on newly cleared land [30].

The time required to clear the PA is underestimated because the time required to move machines between areas is not accounted for, nor is the fact that machine productivity may be lower during NW due to frozen grounds. Machines are also considered perfectly allocated (although they could be run at higher duty cycles, this would also increase maintenance and fuel burn).

Limitations related to the fact that only one cultivar is used include: (i) possible inability to scale up this variety to cover the whole world, and (ii) insufficient wheat production caused by the cultivar's susceptibility to pest attacks. Production could increase by breeding cultivars more suitable for the impending future climate or by optimising planting date for each year of NW would increase yield over time (though given the high levels of uncertainty, this would not be done accurately). Finally, the model might be underestimating wheat production because of four factors: (i) there could be economically viable locations within grid cells with an average wheat

yield < 1000 kg/ha/year; (ii) precipitation might increase due to greater transpiration of the well-suited crops versus the default non-relocated vegetation, (iii) better adapted crops could be used, and (iv) urban areas could have some crop production [46].

5. Conclusion

The cropland expansion plan via conversion of other land types seems to be a viable food-providing system during a catastrophe like NW. In the scenario where equipment trade is maintained and equipment is shared globally, cropland area can be expanded by 515 Mha in just 12 months, leading to a cumulative wheat production of over 6 billion t of wheat over 7 years. If machinery trade collapses after the catastrophe, we would be able to globally expand cropland area by 440 Mha, which would allow for the cumulative production of over 4 billion t of wheat over the course of 7 years. In the scenario where the EP is used to supplement the machinery fleet of some countries, it is possible to expand cropland area by 510 Mha in 7 years, with a cumulative wheat production of over 5 billion t over 7 years. This shows not only it would be able to produce enough wheat to feed over a billion people during a catastrophe, but that maintaining trade working during said catastrophe would accelerate the land clearing process and provide more food to more people. Future work would include uncertainty and sensitivity analysis about different input parameters (annual yield, equipment numbers, other cultivars) and model parameters, researching how this project could be done if electricity/fossil fuel production stops, improving the trade-with-EP scenario to allocate machinery according to the land type most difficult to clear, consider reduction in trade of food or other inputs such as fertiliser, pesticides, seeds, and fuel, and overcoming the stated limitations.

List of Abbreviations

ALLFED	Alliance to Feed the Earth in Disasters
ASRS	Abrupt sunlight-reduction scenario
B	Barren
CGIAR	Consultative Group on International Agricultural Research
DBH	Diameter at breast height
DSSAT	Decision-Support System for Agrotechnology Transfer
EP	Export pool
EPS	Export-pool scenario
F1	Forest with trees aged 1 - 10 years-old
F2	Forest with trees aged 11 - 20 years-old
F3	Forest with trees aged 21 - 30 years-old
FAO	Food and Agriculture Organisation
FAOSTAT	Global Food and Agriculture Statistics of FAO
GFAD	Global forest age dataset
GFRA	Global Forest Resources Assessment
GTS	Global-trade scenario
H	Herbaceous vegetation
HBS	Herbaceous vegetation, barren land, and shrubland
IFPRI	International Food Policy Research Institute

NTS	No-trade scenario
NW	Nuclear winter
PA	Productive area
S	Shrubland
SI	Site index
SOC	Soil organic carbon

Supplementary materials

The following supporting information can be downloaded at: insert link, Equation S1: DBH as a function of tree age; Equation S2: Single tree total volume for *Brachystegia* tree; Equation S3: Single tree total volume for *Julbernardia* tree; Equation S4: SI equation for white spruce trees in Canada; Equation S5: SI equation for beech in Chile; Equation S6: SI equation for *Pinus radiata* in Spain; Equation S7: SI equation for *Pinus kesiya* in the Philippines; Equation S8: SI equation for *Eucalyptus diversicolor* in Australia; Equation S9: DBH equation for eucalyptus. Equation S10: Tree trunk volume; Equation S11: Tree crown volume; Equation S12: Stump hole volume; Table S1: Land clearing tasks and respective equipment; Table S2: Equipment loaned to the EP; Table S3: Countries that receive machinery from the EP, their PA, and what percentage of the total EP they receive; Table S4: Total wheat production in countries that receive machinery from the EP in the NTS and EPS scenarios; Table S5: Parameters for Equation S1; Table S6: Measurements of the representative trees of each continent.

Acknowledgements

The crop model was a product of IFPRI/CGIAR and ALLFED collaboration (https://github.com/allfed/mink). The authors would like to thank Ricky Robertson at IFPRI, Dr. Benjamin Poulter at NASA, and Nicholas Lam, Baxter Williams, and Dr. Campbell Harvey at the University of Canterbury for their help. This research was funded by the Department of Mechanical Engineering at the University of Canterbury and by ALLFED.

Author contributions

L.L.M.: conceptualization, formal analysis, funding acquisition, investigation, methodology, project administration, visualisation, writing - original draft; M.H.: formal analysis, investigation, supervision; M.R.: data curation, investigation, methodology, software, resources, writing - original draft; S.B.: data curation, investigation, methodology, software, resources, writing - original draft; J.D.W.: formal analysis, resources, supervision, visualisation; D.D.: conceptualization, funding acquisition, investigation, methodology, project administration, resources, supervision, writing - original draft.

Funding sources

This research was funded in part by the Alliance to Feed the Earth in Disasters (ALLFED). Luísa L. Monteiro was funded as a PhD student by the Department of Mechanical Engineering at the University of Canterbury.

References

[1] D. Denkenberger and J. M. Pearce, *Feeding everyone no matter what: managing food security after global catastrophe*. London: Academic Press, 2015.

[2] A. Pham, J. B. García Martínez, V. Brynych, R. Stormbjorne, J. M. Pearce, and D. C. Denkenberger, “Nutrition in abrupt sunlight reduction scenarios: envisioning feasible balanced diets on resilient foods,” *Nutrients*, vol. 14, no. 3, p. 492, Jan. 2022, doi: 10.3390/nu14030492.

[3] A. M. Barrett, S. D. Baum, and K. Hostetler, “Analyzing and reducing the risks of inadvertent nuclear war between the United States and Russia,” *Sci. Glob. Secur.*, vol. 21, no. 2, pp. 106–133, May 2013, doi: 10.1080/08929882.2013.798984.

[4] M. Boyd and N. Wilson, “Island refuges for surviving nuclear winter and other abrupt sunlight-reducing catastrophes,” *Risk Anal.*, vol. 43, no. 9, 2023, doi: 10.1111/risa.14072.

[5] A. Robock, “Nuclear winter,” *WIREs Clim. Change*, vol. 1, no. 3, pp. 418–427, May 2010, doi: 10.1002/wcc.45.

[6] J. Coupe, C. G. Bardeen, A. Robock, and O. B. Toon, “Nuclear winter responses to nuclear war between the United States and Russia in the whole atmosphere community climate Model Version 4 and the Goddard Institute for space studies ModelE,” *J. Geophys. Res. Atmospheres*, vol. 124, no. 15, 2019, doi: 10.1029/2019JD030509.

[7] D. J. Winstead and M. G. Jacobson, “Forest resource availability after nuclear war or other sun-blocking catastrophes,” *Earths Future*, vol. 10, no. 7, 2022, doi: 10.1029/2021EF002509.

[8] L. Xia *et al.*, “Global food insecurity and famine from reduced crop, marine fishery and livestock production due to climate disruption from nuclear war soot injection,” *Nat. Food*, vol. 3, no. 8, 2022, doi: 10.1038/s43016-022-00573-0.

[9] D. Denkenberger, D. D. Cole, M. Abdelkhaliq, M. Griswold, A. B. Hundley, and J. M. Pearce, “Feeding everyone if the sun is obscured and industry is disabled,” *Int. J. Disaster Risk Reduct.*, vol. 21, 2017, doi: 10.1016/j.ijdrr.2016.12.018.

[10] J. Jägermeyr *et al.*, “A regional nuclear conflict would compromise global food security,” *Proc. Natl. Acad. Sci.*, vol. 117, no. 13, pp. 7071–7081, Mar. 2020, doi: 10.1073/pnas.1919049117.

[11] M. Rivers *et al.*, *Food system adaptation and maintaining trade could mitigate global famine in abrupt sunlight reduction scenarios*. 2024. doi: 10.5281/zenodo.11484350.

[12] F. U. Jehn *et al.*, “Seaweed as a resilient food solution after a nuclear war,” *Earths Future*, vol. 12, no. 1, p. e2023EF003710, 2024, doi: 10.1029/2023EF003710.

[13] K. A. Alvarado, A. Mill, J. M. Pearce, A. Vocaet, and D. Denkenberger, “Scaling of greenhouse crop production in low sunlight scenarios,” *Sci. Total Environ.*, vol. 707, p. 136012, Mar. 2020, doi: 10.1016/j.scitotenv.2019.136012.

[14] J. Throup, J. B. García Martínez, B. Bals, J. Cates, J. M. Pearce, and D. C. Denkenberger, “Rapid repurposing of pulp and paper mills, biorefineries, and breweries for lignocellulosic sugar production in global food catastrophes,” *Food Bioprod. Process.*, vol. 131, pp. 22–39, Jan. 2022, doi: 10.1016/j.fbp.2021.10.012.

[15] J. B. García Martínez, J. M. Pearce, J. Throup, J. Cates, M. Lackner, and D. C.

Denkenberger, “Methane single cell protein: potential to secure a global protein supply against catastrophic food shocks,” *Front. Bioeng. Biotechnol.*, vol. 10, 2022, doi: 10.3389/fbioe.2022.906704.
[16] T. Fist, A. A. Adesanya, D. Denkenberger, and J. M. Pearce, “Global distribution of forest classes and leaf biomass for use as alternative foods to minimize malnutrition,” *World Food Policy*, vol. 7, no. 2, pp. 128–146, 2021, doi: 10.1002/wfp2.12030.
[17] J. B. García Martínez, K. A. Alvarado, and D. C. Denkenberger, “Synthetic fat from petroleum as a resilient food for global catastrophes: Preliminary techno-economic assessment and technology roadmap,” *Chem. Eng. Res. Des.*, vol. 177, pp. 255–272, Jan. 2022, doi: 10.1016/j.cherd.2021.10.017.
[18] N. Wilson, B. Payne, and M. Boyd, “Mathematical optimization of frost resistant crop production to ensure food supply during a nuclear winter catastrophe,” *Sci. Rep.*, vol. 13, no. 1, p. 8254, May 2023, doi: 10.1038/s41598-023-35354-7.
[19] A. S. Cohn, J. Gil, T. Berger, H. Pellegrina, and C. Toledo, “Patterns and processes of pasture to crop conversion in Brazil: Evidence from Mato Grosso State,” *Land Use Policy*, vol. 55, pp. 108–120, Sep. 2016, doi: 10.1016/J.LANDUSEPOL.2016.03.005.
[20] FAO, *Global Forest Resources Assessment 2020: Main report*. Rome, Italy: FAO, 2020. doi: 10.4060/ca9825en.
[21] H. Miller, J. Mulhall, L. Pfau, R. Palm, and D. Denkenberger, “Can foraging for earthworms significantly reduce global famine in a catastrophe?,” *Biomass*, vol. 4, pp. 765–783, Jul. 2024, doi: 10.3390/biomass4030043.
[22] D. Nelson, A. Turchin, and D. Denkenberger, “Wood gasification: a promising strategy to extend fuel reserves after global catastrophic electricity loss,” *Biomass*, vol. 4, no. 2, Art. no. 2, Jun. 2024, doi: 10.3390/biomass4020033.
[23] X. Wei, M. Shao, W. Gale, and L. Li, “Global pattern of soil carbon losses due to the conversion of forests to agricultural land,” *Sci. Rep.*, vol. 4, Feb. 2014, doi: 10.1038/srep04062.
[24] A. Don, J. Schumacher, and A. Freibauer, “Impact of tropical land-use change on soil organic carbon stocks – a meta-analysis,” *Glob. Change Biol.*, vol. 17, no. 4, pp. 1658–1670, 2011, doi: 10.1111/j.1365-2486.2010.02336.x.
[25] X.-L. Zhang *et al.*, “Converting alfalfa pasture into annual cropland achieved high productivity and kept soil organic carbon in a semiarid area,” *Land Degrad. Dev.*, vol. 32, no. 3, pp. 1478–1486, 2021, doi: 10.1002/ldr.3808.
[26] Z. Yi, M. Wang, and C. Zhao, “Desert soilization: The concept and practice of making deserts bloom,” *The Innovation*, vol. 3, no. 1, p. 100200, Jan. 2022, doi: 10.1016/j.xinn.2021.100200.
[27] A. R. Peerzada, “The innovation turning desert sand into farmland,” *BBC News*, May 03, 2018. Accessed: Jan. 18, 2024. [Online]. Available: https://www.bbc.com/news/business-43962688
[28] J. E. Tierney, F. S. R. Pausata, and P. B. deMenocal, “Rainfall regimes of the Green Sahara,” *Sci. Adv.*, vol. 3, no. 1, p. e1601503, Jan. 2017, doi: 10.1126/sciadv.1601503.
[29] R. D. Robertson, *Mink: Details of a global gridded crop modeling system*. Washington, D.C.: International Food Policy Research Institute (IFPRI), 2017. [Online]. Available: http://ebrary.ifpri.org/cdm/ref/collection/p15738coll2/id/131406
[30] C. Müller *et al.*, “The Global Gridded Crop Model Intercomparison phase 1 simulation dataset,” *Sci. Data*, vol. 6, no. 1, p. 50, May 2019, doi: 10.1038/s41597-019-0023-8.
[31] International Food Policy Research Institute (IFPRI) and International Institute For Applied Systems Analysis (IIASA), “Global Spatially-Disaggregated Crop Production Statistics Data for 2005 Version 3.2.” Harvard Dataverse, 2015. doi: 10.7910/DVN/DHXBJX.
[32] *Caterpillar Performance Handbook*. in 49, no. SEBD0351-49. Peoria, Ill.: Caterpillar Tractor Co., 2019.

[33] “Trees outside forests - Towards a better awareness,” Food and Agriculture Organization. Accessed: May 27, 2024. [Online]. Available: https://www.fao.org/4/y2328e/y2328e03.htm
[34] The CAT Rental Store, “Equipment needed for land clearing | The CAT rental store.” Accessed: Jan. 17, 2024. [Online]. Available: https://www.catrentalstore.com/en_US/blog/equipment-land-clearing.html
[35] G. P. Castro, J. R. Malinovski, L. Nutto, and R. A. Malinovski, “Machinery and Equipment in Harvesting,” in *Tropical Forestry Handbook*, M. Köhl and L. Pancel, Eds., Berlin, Heidelberg: Springer Berlin Heidelberg, 2015, pp. 1–41. doi: 10.1007/978-3-642-41554-8_183-1.
[36] “How much can a skid steer mulcher clear? - Skid Pro Attachments.” Accessed: Oct. 01, 2024. [Online]. Available: https://skidpro.com/how-much-can-clear-in-a-day/
[37] D. Tiernan, G. Zeleke, P. M. O. Owende, C. L. Kanali, J. Lyons, and S. M. Ward, “Effect of working conditions on forwarder productivity in cut-to-length timber harvesting on sensitive forest sites in Ireland,” *Biosyst. Eng.*, vol. 87, no. 2, pp. 167–177, Feb. 2004, doi: 10.1016/j.biosystemseng.2003.11.009.
[38] R. Jiroušek, R. Klvac, and A. Skoupý, “Productivity and costs of the mechanised cut-to-length wood harvesting system in clear-felling operations,” *J. For. Sci.*, vol. 53, pp. 476–482, Oct. 2007, doi: 10.17221/2088-JFS.
[39] M. Ghaffariyan, “Reviewing productivity studies of skidders working in coniferous forests and plantations,” *Silva Balc.*, vol. 21, pp. 83–89, Oct. 2020, doi: 10.3897/silvabalcanica.21.e56071.
[40] B. Andersson and C. M. Evans, “Harvesting overmature aspen stands in Central Alberta,” 1996.
[41] B. Poulter *et al.*, “The global forest age dataset and its uncertainties (GFADv1.1),” *NASA National Aeronautics and Space Administration*. PANGAEA, 2019. doi: 10.1594/PANGAEA.897392.
[42] T. W. Crowther *et al.*, “Mapping tree density at a global scale,” *Nature*, vol. 525, no. 7568, pp. 201–205, Sep. 2015, doi: 10.1038/nature14967.
[43] “WHEAT in the World,” CGIAR. Accessed: May 27, 2024. [Online]. Available: https://archive.wheat.org/wheat-in-the-world/
[44] “Production of wheat worldwide 2023/24,” Statista. Accessed: May 21, 2024. [Online]. Available: https://www.statista.com/statistics/267268/production-of-wheat-worldwide-since-1990/
[45] S. Gbegbelegbe *et al.*, “Baseline simulation for global wheat production with CIMMYT mega-environment specific cultivars,” *Field Crops Res.*, vol. 202, pp. 122–135, Feb. 2017, doi: 10.1016/j.fcr.2016.06.010.
[46] M. Boyd and N. Wilson, *Combining urban and peri-urban agriculture for resilience to global catastrophic risks disrupting trade: quantified case study of a median-sized city*. 2024. doi: 10.21203/rs.3.rs-4590974/v1.

Supplement

Determination of tree measurements

It is important for these equations to be site specific because environment is one of the main factors influencing tree growth. Therefore, the height of each representative tree was determined using site index equations. Site index (SI) corresponds to the average height achieved by trees of a given species at some base age [1].

In Africa, the 2 most common tree genera are *Brachystegia* (Bc) and *Julbernardia* (Jb). Malengue et al. [2] developed SI equations for both in the Angolan miombo woodlands, so **Equation S1** was used to estimate the DBH of the trees according to tree age, a relationship characterized by a fitted sigmoidal curve based on the mean diameter of the trees, using the parameters in **Table S5** (*a*, *m*, and t_{max} which correspond to the upper asymptote, growth rate, and time of maximum growth). To calculate the height (*h*) of these trees, we used the models developed by Abbot et al. [3] to calculate the volume of the trees as a function of the diameter at breast height (DBH). **Equations S2 and S3** were used to calculate the volume of Bc and Jb, respectively, and then the height was calculated using the formula for the volume of a cylinder. According to the GFRA 2020 report [4], the distribution ratio of Jb to Bc is approximately 1:2, so the measurements for trees in Africa were calculated using a weighted average of the measurements for Bc (70%) and Jb (30%).

$$DBH = a/\left\{1 + \left[m \times exp(t_{max} \times age)\right]\right\} \quad \text{Equation S1}$$

$$log_{10}V_{Brachystegia} = -3.85 + 2.49 log_{10}DBH \quad \text{Equation S2}$$

$$log_{10}V_{Julbernardia} = -4.00 + 2.65 log_{10}DBH \quad \text{Equation S3}$$

The most common tree genus in North America is *Picea*, while in South America it is *Nothofagus*. An average of the measurements of these two trees at different ages was used to estimate the measurements of trees in the American continent. Wang et al. [5] examined the SI of white spruce trees in Canada, and **Equation S4** was used to estimate the height according to age, for an SI of 18 m. For South America, SI curves for beech in Chile were developed by Esse et al. [6] to determine height according to age, assuming an SI of 19 m, according to **Equation S5**.

$$h = 1.3 + (18 - 1.3) \times \frac{\{1+exp[9.56-1.451ln(50)-1.236ln(18-1.3)]\}}{\{1+exp[9.565-1.451ln(age)-1.236ln(18-1.3)]\}} \quad \text{Equation S4}$$

$$h = 36.677176 \times \left\{1 - \left[1 - (19/36.677176)^{1/1.44887}\right]^{age/35}\right\}^{1.44887} \quad \text{Equation S5}$$

Pinus is the most common tree genus in both Europe and Asia. The SI models developed by Molina-Valero et al. [7] for pine trees in the north of Spain were used to estimate the height of trees in Europe, assuming an SI of 21 m for base age of 20 years, and a base

DBH of 30 cm, according to **Equation S6**. For pine trees in Asia, height was calculated using equation 4 from Lumbres et al. [8], assuming an SI of 18 m for base age of 25 years, according to **Equation S7**.

$$h = 48/\left[1 + \left(\frac{8059}{48} \times age^{-1.62}\right)\right] \quad \text{Equation S6}$$

$$h = 18 \times \left[\frac{1-exp(-0.0419\times age)}{1-exp(-0.0419\times 25)}\right]^{0.8823} \quad \text{Equation S7}$$

Rayner [9] examined the SI of *Eucalyptus* in Australia, and **Equation S8** was used to calculate the height of trees in Oceania according to age, for an SI of 30 m and base age of 50 years. The diameter of these trees was estimated according to **Equation S9**.

$$h = 30 \times \left[\frac{1-exp\left(-0.0625\times age^{0.8956}\right)}{1-exp\left(-0.0625\times 50^{0.8956}\right)}\right]^{1.233} \quad \text{Equation S8}$$

$$DBH = age^{1/0.98} \quad \text{Equation S9}$$

The age of a tree can be determined by multiplying its DBH by the growth factor, a species-dependent variable. For the Americas, the growth factors for *Picea* and *Nothofagus* were 4.5 and 6, respectively. For pine trees in Asia and Europe, growth factors of 5 and 4.5 were used, based on the growth factor of white pine and Austrian pine, respectively [10]. The measurements from each representative tree are shown in **Table S6**.

The volume of the tree trunks according to **Equation S10**, where H corresponds to height minus 0.5 m, which the authors assumed to be the average stump height.

$$Tree\ volume\ (m^3) = \pi \cdot \left(\frac{DBH}{2}\right)^2 \cdot h \quad \text{Equation S10}$$

Tree crown volume is calculated to know how much slash the felled trees leave behind. We assumed the tree crown shape is comparable to a cone, and its solid volume can be calculated using **Equation S11**, where CR corresponds to crown radius and CH to crown height. Tree crowns carry branches and foliage with empty space between them, so the volume has to account for the gap factor (GF), which we assumed to be 0.9674, an average of the values determined by Zhu et al. [11]. Lockhart et al. developed linear models to predict CR from DBH in different tree species, which were used to calculate the CR of the trees in this project [12]. Crown height was assumed to correspond to 48% of the total tree height, the average of CR measurements of different trees documented by Temesgen et al. [13].

$$Tree\ crown\ volume\ (m^3) = \frac{1}{3} \cdot \pi \cdot CR^2 \cdot CH \cdot (1 - GF) \quad \text{Equation S11}$$

According to Koren et al. [14], the volume of a tree stump corresponds to approximately 5.7% of the total tree volume, which was used to calculate the tree stump volume. Stump removal leaves behind holes in the ground which will be filled by excavators. **Equation S12** is used to predict how much soil is required to fill these holes, assuming a hole with a depth of 0.9 meters was dug and a minimum safe distance from the tree of 1.5 times the DBH of the tree was used.

$$Stump\ hole\ volume\ (m^3) = \pi \cdot (1.5 \cdot DBH)^2 \cdot 0.9 \qquad \text{Equation S12}$$

Tables

Table S1 - Land clearing tasks and respective equipment

Task	Equipment
Leveling and debris removal	Skid steer loaders Compact track loaders Dozers
Tree shearing	Skid steer loaders Compact track loaders Dozers
Log collection	Skidders Forwarders

Table S2 - Equipment loaned to the export pool (EP)

Continent	Number of countries loaning equipment	Number of loaned pieces of construction equipment	Number of loaned pieces of forestry equipment
Africa	16	153,250	28,752
America	7	236,485	48,455
Asia	24	1,558,564	41,813
Europe	30	1,960,367	222,209
Oceania	3	22,293	11,933
Total	80	3,930,958	353,163

Table S3 - Countries that receive machinery from the EP, their productive area (PA), and what percentage of the total EP they receive

Continent	Country	Area (Mha)	Fraction of machinery
Africa	Angola	34	9.85%
	Benin	2.9	0.85%
	Burkina Faso	3.4	0.97%
	Central African Republic	10	2.90%

	Côte d'Ivoire	5.8	1.66%
	Cameroon	5.9	1.71%
	Democratic Republic of Congo	34	9.88%
	Congo	4.6	1.33%
	Guinea	7.8	2.24%
	Liberia	0.5	0.14%
	Lesotho	0.8	0.23%
	Madagascar	14	4.00%
	Mali	5.6	1.61%
	Mozambique	14	4.11%
	Malawi	1.4	0.41%
	Sierra Leone	0.7	0.19%
	Chad	4.7	1.34%
	Togo	0.8	0.23%
	Tanzania	17	4.81%
	Zambia	19	5.40%
	Zimbabwe	3.8	1.09%
America	Argentina	29	8.28%
	Bolivia	17	5.04%
	Colombia	12	3.58%
	Guyana	1	0.23%
	Peru	7	2.04%
	Paraguay	10	2.87%
	Suriname	1	0.19%
	Venezuela	12	3.39%
Oceania	Australia	66	19.04%
	Papua New Guinea	1	0.39%

Table S4 - Total wheat production in countries that receive machinery from the EP in the no-equipment-trade (NTS) and equipment trade with EP (EPS) scenarios

		Total wheat production over 7 years (Mt)	
Continent	**Country**	**No equipment trade**	**Equipment trade with EP**
Africa	Angola	114	234
	Benin	13	22
	Burkina Faso	22	27

	Central African Republic	3	48
	Côte d'Ivoire	39	44
	Cameroon	38	46
	Democratic Republic of Congo	139	301
	Congo	24	33
	Guinea	29	63
	Liberia	3	4
	Lesotho	4	5
	Madagascar	50	217
	Mali	23	42
	Mozambique	38	157
	Malawi	16	21
	Sierra Leone	1	5
	Chad	24	34
	Togo	6	7
	Tanzania	124	174
	Zambia	75	195
	Zimbabwe	39	44
America	Argentina	224	245
	Bolivia	92	195
	Colombia	140	158
	Guyana	13	13
	Peru	79	80
	Paraguay	68	91
	Suriname	5	6
	Venezuela	136	163
Oceania	Australia	631	678
	Papua New Guinea	12	13
Total		2,223	3,365

Table S5 - Parameters for Equation S1

Parameters based on the Caala site		
Tree genus	*Brachystegia*	*Julbernardia*
a	32.666	27.643

m	6.163	6.096
t_{max}	0.091	0.132

Table S6 - Measurements of the representative trees of each continent

		DBH (cm)			Height (m)		
Continent	**Genus of representative tree**	**1 - 10 years**	**11 - 20 years**	**21 - 30 years**	**1 - 10 years**	**11 - 20 years**	**21 - 30 years**
Africa	*Brachystegia and Julbernardia*	7	13	21	4	7	8
Americas	*Picea and Nothofagus*	2	7	12	2	5	9
Asia	*Pinus*	3	8	13	6	13	18
Europe	*Pinus*	3	9	14	4	16	25
Oceania	*Eucalyptus*	5	16	27	6	15	22

References

[1] “How to determine site index in silviculture - Participant’s Workbook.” Forest Renewal BC, 1999. Accessed: Sep. 11, 2024. [Online]. Available: https://www2.gov.bc.ca/assets/gov/farming-natural-resources-and-industry/forestry/silviculture/training-modules/sicourse.pdf

[2] A. Malengue, D. Ariza, R. Navarro-Cerrillo, A. M. Cachinero-Vivar, and J. Camarero, “Ring data provide management clues and pinpoint climate drivers of growth in two species of Miombo trees (Brachystegia spiciformis, Julbernardia paniculata),” *Dendrochronologia*, vol. 81, p. 126117, Jul. 2023, doi: 10.1016/j.dendro.2023.126117.

[3] P. Abbot, J. Lowore, and M. Werren, “Models for the estimation of single tree volume in four Miombo woodland types,” *For. Ecol. Manag.*, vol. 97, no. 1, pp. 25–37, Sep. 1997, doi: 10.1016/S0378-1127(97)00036-4.

[4] FAO, *Global Forest Resources Assessment 2020: Main report*. Rome, Italy: FAO, 2020. doi: 10.4060/ca9825en.

[5] G. G. Wang, P. L. Marshall, and K. Klinka, “Height growth pattern of white spruce in relation to site quality,” *For. Ecol. Manag.*, vol. 68, no. 2, pp. 137–147, Oct. 1994, doi: 10.1016/0378-1127(94)90041-8.

[6] C. Esse, P. J. Donoso, V. Gerding, C. Navarro, and F. Encina-Montoya, “Modelling dominant height and site index in different edaphoclimatic zones of Nothofagus dombeyi secondary forest in the Andes of south-central Chile,” *South. For. J. For. Sci.*, vol. 76, no. 4, pp. 221–228, Oct. 2014, doi: 10.2989/20702620.2014.956026.

[7] J. Molina-Valero, U. Diéguez-Aranda, J. Álvarez-González, F. Castedo-Dorado, and C. Pérez Cruzado, “Assessing site form as an indicator of site quality in even-aged Pinus radiata D. Don stands in north-western Spain,” *Ann. For. Sci.*, vol. 76, p. 113, Dec. 2019, doi: 10.1007/s13595-019-0904-1.

[8] R. Lumbres, Y. Lee, Y. Seo, and F. Calora Jr, “Development of site index curves for Pinus kesiya in the Philippines,” *South. For. J. For. Sci.*, vol. 74, no. 2, pp. 115–120, Jul. 2012, doi: 10.2989/20702620.2012.701441.

[9] M. E. Rayner, “Site index and dominant height growth curves for regrowth karri (Eucalyptus diversicolor F. Muell.) in south-western Australia,” *For. Ecol. Manag.*, vol. 44, no. 2, pp. 261–283, Nov. 1991, doi: 10.1016/0378-1127(91)90013-L.

[10] “Estimate Tree Age | the Intown Hawk.” Accessed: Aug. 12, 2024. [Online]. Available: https://intownhawk.com/estimate-tree-age/
[11] Y. Zhu *et al.*, “A reinterpretation of the gap fraction of tree crowns from the perspectives of computer graphics and porous media theory,” *Front. Plant Sci.*, vol. 14, 2023, doi: 10.3389/fpls.2023.1109443.
[12] B. R. Lockhart, R. C. Weih, and K. M. Smith, “Crown radius and diameter at breast height relationships for six bottomland hardwood species,” *J Ark Acad Sci*, vol. 59, Jan. 2005.
[13] H. Temesgen, V. LeMay, and S. J. Mitchell, “Tree crown ratio models for multi-species and multi-layered stands of southeastern British Columbia,” *For. Chron.*, vol. 81, no. 1, pp. 133–141, Feb. 2005, doi: 10.5558/tfc81133-1.
[14] M. Koreň, Ľ. Scheer, R. Sedmák, and M. Fabrika, “Evaluation of tree stump measurement methods for estimating diameter at breast height and tree height,” *Int. J. Appl. Earth Obs. Geoinformation*, vol. 129, p. 103828, May 2024, doi: 10.1016/j.jag.2024.103828.